Integrated Endoscopic System Based on Optical Imaging and Hyperspectral Data Analysis for Colorectal Cancer Detection

RYUICHI KUMASHIRO[1,2], KOZO KONISHI[2], TOHRU CHIBA[3], TOMOHIKO AKAHOSHI[4], SHOTARO NAKAMURA[5], MASAHARU MURATA[4], MORIMASA TOMIKAWA[1,2], TAKAYUKI MATSUMOTO[5], YOSHIHIKO MAEHARA[2] and MAKOTO HASHIZUME[1,5]

[1]*Center for Integration of Advanced Medicine, Life Science and Innovative Technology, Kyushu University, Fukuoka, Japan;*
[2]*Department of Surgery and Science, Graduate School of Medical Sciences, Kyushu University, Fukuoka, Japan;*
[3]*PENTAX Lifecare Division, Hoya Corporation, Tokyo, Japan;*
[4]*Department of Disaster and Emergency Medicine, Graduate School of Medical Sciences, Kyushu University, Fukuoka, Japan;*
[5]*Second Department of Internal Medicine Kyushu University Hospital, Fukuoka, Japan*

Abstract. *Background/Aim: Two-dimensional hyperspectral data systems with enhanced area detection and diagnostic abilities are now available in gastrointestinal endoscopy for colorectal cancer. We evaluated a new hyperspectral system for diagnosis of colorectal cancer. Patients and Methods: A resected-specimen spectrum observation module (stereoscopic macroscope, hyperspectral camera, and xenon lamp) was used to evaluate 21 resected colorectal cancer specimens (ex vivo experiment). A colonoscopy spectrum observation module (imaging fiberscope and hyperspectral camera) was used to perform 24 colonoscopic spectroscopy evaluations (in vivo experiment). Results: An approximately 525-nm increase in spectral absorption occurred between normal mucosa and adenoma, with a tendency toward decreased absorption rates with aggravation of other tumor types. In vivo discrimination between tumorous and non-tumorous tissues showed 72.5% sensitivity and 82.1% specificity. Conclusion: This in vivo hyperspectral diagnostic system showed that reflectance spectra intensity may discriminate between normal and abnormal colonic mucosa.*

Correspondence to: Makoto Hashizume, PD, Department of Disaster and Emergency Medicine, Graduate School of Medical Sciences, Kyushu University 3-1-1, Maidashi, Higashi-ku, Fukuoka 812-8582, Japan. Tel: +81 926426222, Fax: +81 926426222, e-mail: mhashi@dem.med.kyushu-u.ac.jp

Key Words: Hyperspectral analysis, optical biopsy, reluctant spectroscopy, colonoscopy.

Colorectal cancer remains the third leading cause of death in Western countries and Japan (1, 2), underscoring the need for more effective prevention strategies. Early detection and tretment are important to improve the prognosis of this cancer, and gastrointestinal endoscopy plays an important role in both diagnosis and treatment. The recent improvement in the diagnostic ability of gastrointestinal endoscopy is due to the progress of optical technology. Magnifying endoscopes enable cellular and subcellular observation, and narrow-band imaging enables specific depiction of lesions. However, both techniques require a final macroscopic diagnosis by the examiner; thus, difficulty remains in the relative diagnosis of these tumors. As techniques of objective observation, spectroscopic methods such as fluorescence, Raman, and infra-red spectroscopy have been intensively studied for cancer diagnosis in the past two decades (3). Optical analysis techniques for characterization of spectral data have also been reported (4).

Conventional spectral measurements using endoscopy have been performed with single or multiple optical fibers onto which the reflection light from the tissue surface is transmitted. Acquisition of spectral data with these systems is limited by the number of fibers and detectors. Single-fiber systems have some difficulties in terms of practical use, especially in detecting the spectral data of several positions simultaneously and recognizing their positions (5).

Two-dimensional spectral data called "hyperspectral data" have recently become available (3). These data include spectral information in each pixel that is handled as images of any wavelength band (6, 7). Hyperspectral data provide great advantages in supplying diagnostic support information to the endoscopic field. The greatest advantage of these data is their indication of spatial spectrum variation; consequently, area detection and diagnosis that had not been

successful in this field are enabled. In this study, we evaluated the use of our newly developed hyperspectral system for diagnosis of colorectal cancer.

Patients and Methods

Principle of the system. When a material is exposed to light, a part of the light is absorbed or transmitted; the remainder is reflected. The spectrum included in the reflected light varies according to the material.

Hyperspectral cameras (HSCs) can capture the spectral information of the object as an image. Conventional spectrometers measure spectral information for only one area, but the HSC can acquire spectral information of every single pixel of a multipixel image. In the present study, we constructed a resected-specimen spectrum observation module and a colonoscopy spectrum observation module that assumed HSC as an axis and examined these modules clinically. The elements of the HSC system are described below.

Resected-specimen spectrum observation module. The module for observing resected specimens comprised a stereoscopic macroscope (YS05Z; Micronet, Chiba, Japan), an HSC (HSC1700; Eba Japan, Tokyo, Japan), and a xenon lamp (XEF-152S; Kenko, Tokyo, Japan) (Figure 1A). We attached the HSC to the "C mount" of the macroscope and observed resected specimens of colorectal cancer (tumor and normal mucosa). The XEF-152S xenon lamp was employed as the light source for reflectance spectroscopy. Using this module, we acquired spectral data from the image of an identical area obtained by a stereoscopic microscope (Figure 1B, C).

Colonoscopy spectrum observation module. The colonoscopic spectroscopy module used in this study was based on the combination of an imaging fiberscope (FCP-8P; Pentax, Tokyo, Japan) and the HSC1700 (Eba Japan) (Figure 2A). The baby scope (FCP-8P) was placed into the biopsy channel of the mother colonoscope (GIF-H260; Olympus, Tokyo, Japan) to detect the reflectance signal of the colonic mucosa of the patient while undergoing colonoscopic screening. A common xenon lamp (Lucera endoscopy system; Olympus) was employed as the light source for reflectance spectroscopy, primarily because of its adequate brightness. The image of the same area was captured with the camera system equipped in the mother scope. Consequently, hyperspectral data using the HSC1700 and the baby scope system and mother scope images were obtained simultaneously (Figure 2B, C).

Patients and samples. All studies were conducted in accordance with the Institutional Review Board at Kyushu University Hospital. All patients received an adequate explanation about this study from informational material approved by the Institutional Review Board (IRB number: 20-11; July 7, 2008).

Resected-specimen spectrum observation (ex vivo experiment). Using the resected-specimen spectrum observation module and the HSC, we observed 21 resected specimens of colorectal cancer that were collected in the Department of Surgery and Sciences of Kyushu University from 2009 to 2010. The patients comprised of 12 men and 9 women with a mean age of 68 (range=47-82) years. None of the patients had received chemotherapy, eradiation, or immunomodulatory agents before surgery. Among the 21 patients, the tumor location was the ascending colon in 5 (23%), descending colon in 4 (19%), sigmoid colon in 6 (29%), and rectum in 6 (29%). Other clinical findings of the 21 patients are shown in Table I. For observation of the resected specimens, we exposed the target to the xenon light and observed the reflection using the HSC. We extracted data for 10×10 pixels from the portion that was pathologically clear of cancer and used the mean as the HSC data of the cancer. Because the reflection intensity was strongly affected by the reflection angle and the distance between the target and camera, the value was compensated depending on its condition to allow for comparison of the data of each pixel (Figure 3).

Colonoscopic spectroscopy observation (in vivo experiment). Using the colonoscopic spectroscopy module and the HSC, colonoscopic examination was performed in 24 patients at the Second Department

Table I. *Patients' characteristics (in vivo)*.

Parameter	Value
Gender (n=21)	
Female	9
Male	12
Age (years)	
Mean±standard deviation (range)	68.0±8.5 (47-82)
Primary site	
Ascending colon	5
Descending colon	4
Sigmoid colon	6
Rectum	6
Tumor type	
Well differentiated	6
Well to moderately differentiated	5
Moderately differentiated	10

Data are presented as *n* unless otherwise indicated.

Table II. *Patients' characteristics (ex vivo)*.

Parameter	Value
Gender (n=24)	
Female	8
Male	16
Age (years)	
Mean±standard deviation (range)	65±12 (30-85)
Primary site	
Ascending colon	11
Transverse colon	6
Descending colon	1
Sigmoid colon	11
Rectum	11
Lesion type	
Adenocarcinoma	3 (n=3)
Adenoma	30 (n=12)
Hyperplastic polyp	7 (n=5)
Normal mucosa	95 (n=24)

Data are presented as n unless otherwise indicated.

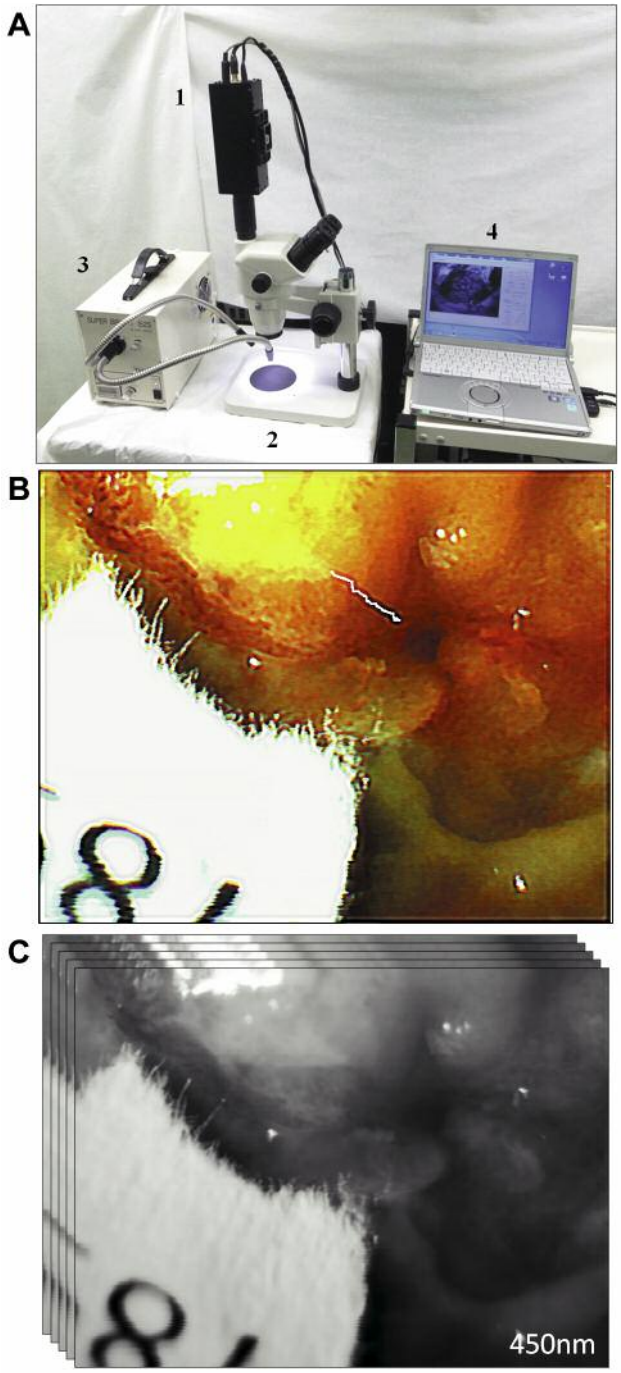

Figure 1. *Spectrum observation module and images (for resected-specimen). (A) 1, Hyperspectral camera; 2, stereoscopic macroscope; 3, xenon light; 4, PC workstation. (B) Stereoscopic microscope image. (C) Hyperspectral camera image.*

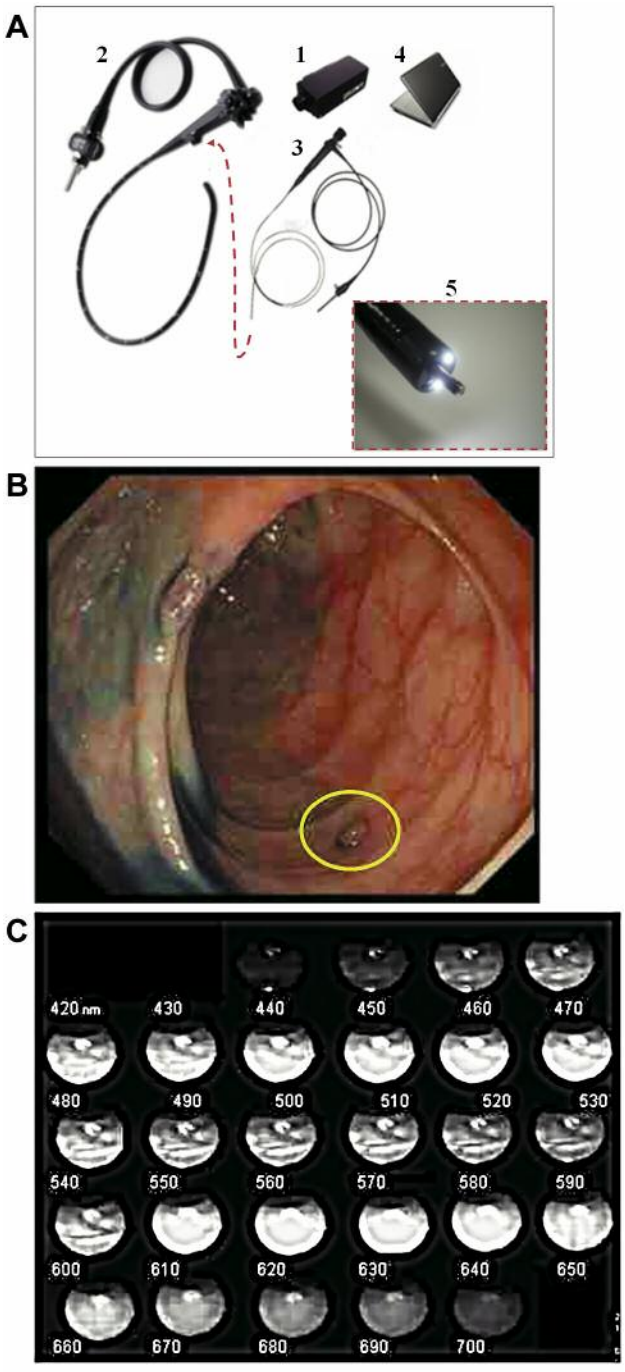

Figure 2. *Spectrum observation module and images (for colonoscopy) (A) 1, Hyperspectral camera; 2, colonoscope; 3, FCP-8P ultra-slim choledochofiberscope; 4, PC workstation; 5, insertion of baby scope through the instrument channel of the colonoscope. (B) Colonoscope image. (C) Hyperspectral camera image.*

of Internal Medicine of Kyushu University from 2008 to 2009. Pathological examination was also performed in patients who underwent a biopsy. The patients comprised of 16 men and 8 women with a mean age of 65 (range=30-85) years. Among the 24 patients, some had multiple lesions and others had normal study findings. We observed 40 lesion sites and 95 normal mucosal sites. The lesion location was the ascending colon in 11 (27.5%), transverse colon in 6 (15.0%), descending colon in 1 (2.5%),

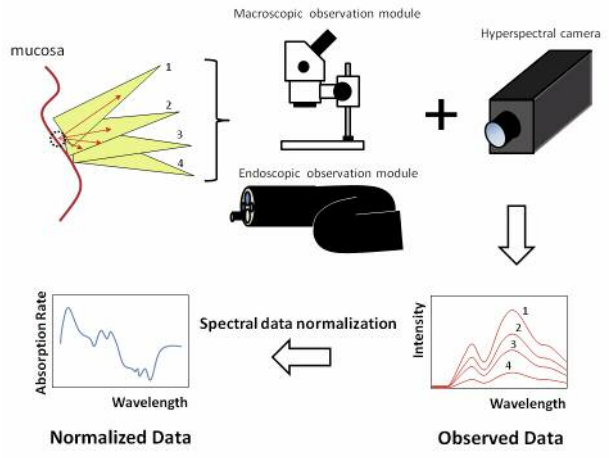

Figure 3. *Spectral data normalization. Outline of the measurement and standardization of hyperspectral camera data.*

sigmoid colon in 11 (27.5%), and rectum in 11 (27.5%). The histological type was categorized as adenocarcinoma, adenoma, hyperplastic polyp, or normal mucosa. Other clinical findings of the 24 patients are shown in Table II.

The scanning time was limited during colonoscopic observation because of intestinal peristalsis and movement of the fiberscope, which was roughly controlled by a freehand technique. Therefore, during endoscopic observation, we confined the scanning area to 200×200 pixels and shortened the scanning time to 5 seconds. The image quality was degraded using this method, but the HSC data were guaranteed. The HSC data were also compensated by the HSC data normalization method, as in the *ex vivo* experiment.

Principle of spectral data analysis. Hyperspectral images contain spectral information of every single pixel of a multipixel image. Therefore, 307,200 places of HSC data are present in 640×480 pixels of a scan. Analysis of all HSC data was redundant, so we extracted data for each 100 pixels (10×10 pixels) of the lesional and normal mucosal sites and adopted the mean as the HSC data characteristic of a case.

Reflectance spectral data were processed to reduce noise, and the 3-point moving average was applied to each spectrum for smoothing. Next, all reflectance spectral data points were reconstructed as 5-nm steps from 405 to 750 nm for analysis (Figure 3).

Equation 1.

O: observed spectrum

R: collected spectrum data of hyperspectral camera

W: reference spectrum

O': normalized spectrum

O: observed spectrum

$\sum_i O(\lambda i)$: total spectrum intensity

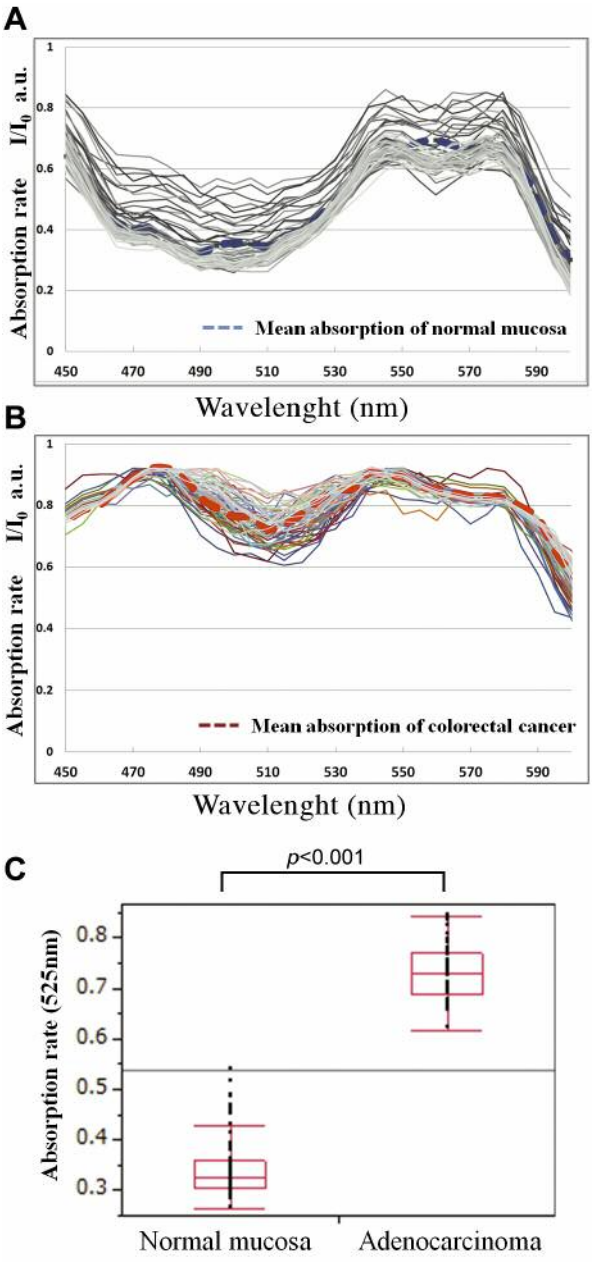

Figure 4. *Spectral data of resected specimen. (A) Absorption rates of normal mucus (ex vivo). (B) Absorption rates of colorectal cancers (ex vivo). (C) Comparison of absorption rate at 525 nm (ex vivo).*

(A)

$$o_{(\lambda i)} = \frac{R(\lambda i)}{W_{(\lambda i)}}$$

$$(i = 1,2,3 \cdots \max)$$

(B)

$$o'_{(\lambda i)} = \left(\frac{O(\lambda 1)}{\sum_i O(\lambda i)}, \frac{O(\lambda 2)}{\sum_i O(\lambda i)}, \cdots \frac{O(\lambda \max)}{\sum_i O(\lambda i)} \right)$$

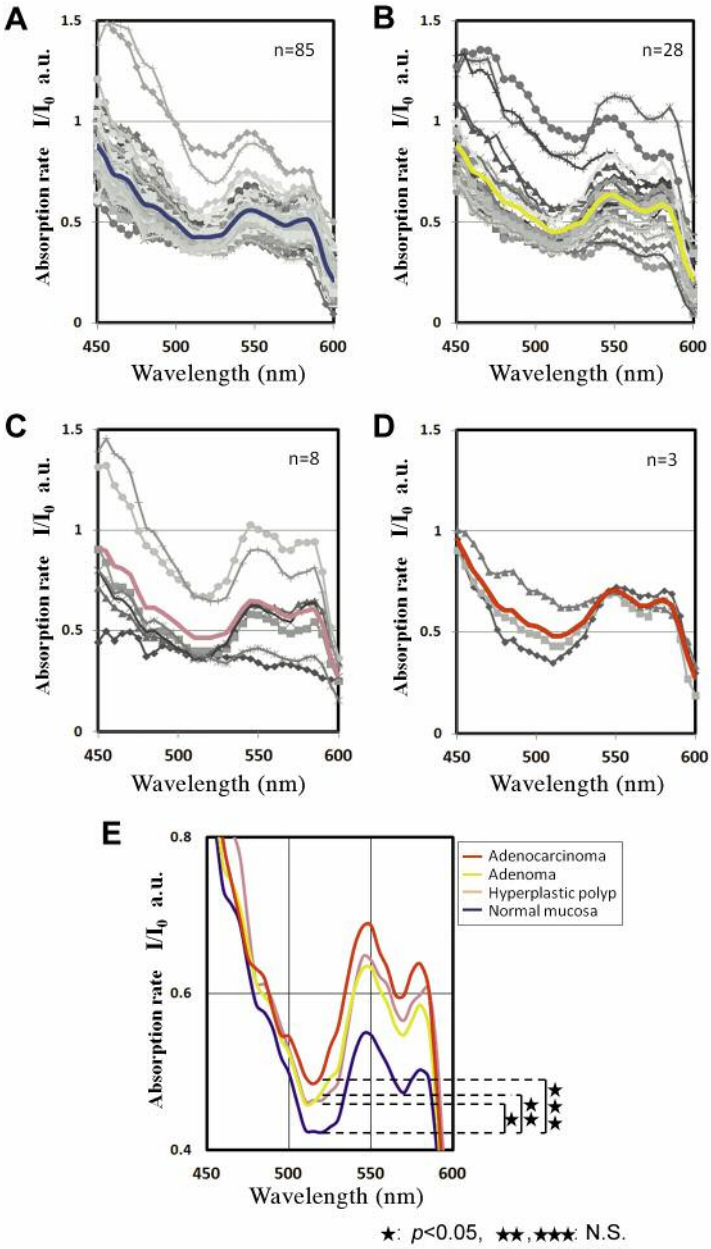

Figure 5. *Spectral data of colonoscopy. (A) Absorption rates of normal mucus (in vivo). (B) Absorption rates of hyperplastic polyps (in vivo). (C) Absorption rates of adenomas (in vivo). (D) Absorption rates of adenocarcinomas (in vivo). (E) Comparison between mean absorption of each group.*

Spectral data normalization. First, geometrical compensation for the surface reflectance was necessary. Because unexpected undulation exists on the surface of human tissue, measured spectral data are affected by the distance and angle of each point.

For recognition of the spectral data, the normalization procedure shown in Equation 1 was employed. Equations 1A and 1B show the transformation of the data. After processing this compensation and treating it as absorbance, a conventional comprehensive study for characterizing turbid media with optical and chemical analysis methods was available in this case.

In this case, for concentration linearity of the components, the data were transformed from refection (%) to absorption ($-\log (I/I_0)$) according to conventional methods. Data are reported as mean (standard deviation). Student's *t*-test was performed for statistical analysis. A *p*-value of <0.05 was considered statistically significant.

Application to real-time tumor mapping and accuracy evaluation of HSC. Based on the results of the resected-specimen spectrum and colonoscopic spectroscopy observations, we evaluated whether our HSC system is useful for tumor mapping, thus discriminating

Table III. *Accuracy evaluation.*

At the specific wavelength (525 nm) (*in vivo*)

	Hyperspectral camera diagnosis		
Pathological diagnosis	Tumor, cancer	Normal mucosa	Total
Tumor, cancer	30	10	40
Normal mucosa	42	53	95

Sensitivity, 75.0%; specificity, 55.8%.

By Pearson correlation analysis (*in vivo*)

	Hyperspectral camera diagnosis		
Pathological diagnosis	Tumor, cancer	Normal mucosa	Total
Tumor, cancer	29	11	40
Normal mucosa	17	78	95

Sensitivity, 72.5%, specificity, 82.1%.

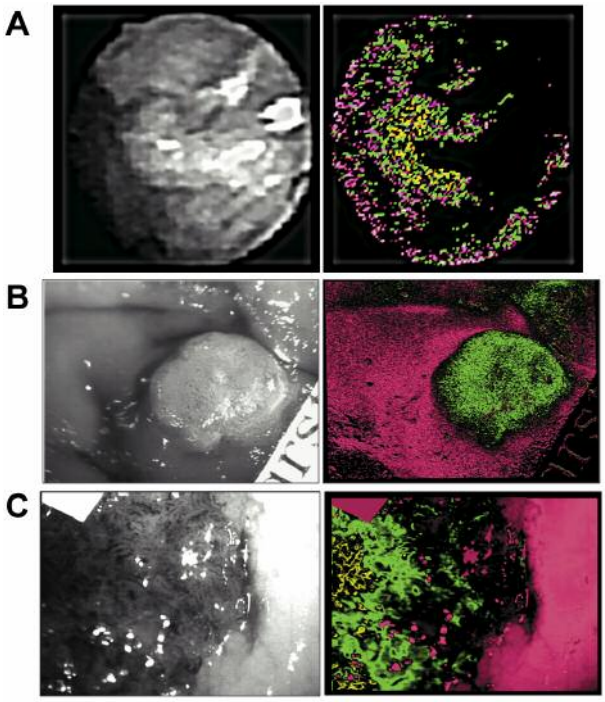

Figure 6. *Real-time tumor mapping. (A) Image of tubular adenoma. Left Hyperspectral image. Right Tumor mapping. (B) Image of well to moderately differentiated adenocarcinoma. Left Hyperspectral image. Right Tumor mapping. (C) Image of moderately differentiated adenocarcinoma. Left Hyperspectral image. Right Tumor mapping.*

tumorous from non-tumorous tissue. We analyzed the results of the *in vivo* and *ex vivo* experiments and identified the tumorous and normal mucosal pathognomonic wavelength change. We then performed tumor mapping based on this wavelength change and inspected its accuracy.

Results

Study 1 (ex vivo experiment). The spectra of colorectal cancer and normal mucosa are shown in Figure 4. Figure 4A corresponds to the absorption of the normal mucosa, and Figure 4b corresponds to the absorption of colorectal cancer. The blue and red dashed lines represent the spectral mean of the tumor mucosa and normal mucosa, respectively. An approximately 525-nm increase in the spectral absorption was observed. The normal mucosal absorption rate was 0.35±0.20 a.u., and that of the cancer portion was 0.75±0.04 a.u. at 525 nm ($p<0.001$).

Study 2 (in vivo experiment). First, we plotted all observed spectral data in the four groups and performed a cyclopedic analysis of the spectrophotometric difference in reflection intensity of the normal mucosa and lesioned part (hyperplastic polyp, adenoma, and adenocarcinoma). Figure 5A-D shows the reflectance spectra from all measured sites, grouped according to the four diagnostic categories. Average spectra are also shown for each diagnostic category (colored line). The average reflection intensity rate of each category was as follows: normal mucosa, 0.43±0.12 a.u.; hyperplastic polyp, 0.46±0.13 a.u.; adenoma, 0.47±0.15 a.u.; and adenocarcinoma, 0.50±0.11 a.u. Figure 5E shows the average spectra for each diagnostic category on the same graph. Analysis at every 5 nm revealed significant differences in the absorption rate at a wavelength of approximately 525 nm between normal mucosa and adenoma ($p<0.05$). In the other groups, a tendency toward a decreased absorption rate with aggravation of the tumor was detected, but there was no significant difference.

Study 3 (accuracy evaluation and real-time tumor mapping) Sensitivity and specificity. In the *in vivo* experiment, we conducted a receiver operating characteristic analysis of the HSC data and set the cut-off value of the absorption rate at 0.41 a.u.

Tumorous and non-tumorous tissues were discriminated with a sensitivity of 75.0% and a specificity of 55.8% (Table III). Conversely, in the *ex vivo* experiment, the normal and tumorous mucosa groups were completely divided at an absorption rate of 0.59 a.u.

However, the classification method should include a featured spectral pattern of the tumor, which depends on its category and stage. Optimization of data collection and the best method of discrimination for each tumor condition remain to be determined in future studies.

Pearson correlation analysis. As one of the most familiar methods for evaluating spectra similarity, Pearson product-moment correlation analysis was employed for the *in vivo* experiment. Twenty data points (435-530 nm each 5-nm interval) for each spectra curve were used to classify normal tissue and lesions, depending on the value of the correlation coefficient. The result of this discrimination was compared with those of the 525-nm point classification. Tumorous and non-tumorous tissues were discriminated with a sensitivity of 72.5% and a specificity of 82.1% (Table III).

Real-time tumor mapping. Based on the spectral characteristics of the proliferative lesions, including the cancers, we performed tumor mapping on the RGB screen. Figure 6 shows the real-time tumor mapping on the RGB screen. These results were significantly correlated with the pathological results.

Discussion

The number of minimally invasive endoscopic approaches for early gastrointestinal cancer is increasing. In particular, the indications for endoscopic resection of early cancer have expanded. We developed a novel *in vivo* reflectance spectroscopy imaging system using hyperspectral data collection and analysis.

A key advantage of using reflectance spectroscopy as a method for diagnosing gastrointestinal diseases is the wide availability and ease of use of the endoscopic instrumentation. Reflectance spectroscopy techniques have shown important applications in key clinical settings, including gastrointestinal ischemia, dysplasia, and neoplasia. Although their use is still in its infancy, early studies have shown tremendous potential for the widespread application of these techniques (3, 8).

Several groups have reported promising results in clinical trials of reflectance spectroscopy for detection of proliferative lesions. Kawabata *et al*. (9) reported that the Raman spectra for gastric cancer specimens differed from those for non-neoplastic specimens, especially at around 1,644 nm. Dhar *et al*. (10) reported differences in the spectral peak intensity in the ultraviolet range (320-400 nm) and in the slope in the near-infrared range (700-800 nm) among normal colonic mucosa, an adenomatous polyp with dysplasia, and adenocarcinoma.

Our findings in colonic tissue compare well with these findings. Concerning the reports by Koenig *et al*. (11) and Ge *et al*. (12), the pathological relationship between the spectral absorbance of hemoglobin (530–580 nm) and 525-nm peak transition will be considered in future research (data not shown).

We also examined the correlation between 525-nm spectral features and blood flow using 2-dimensional correlation analysis. The spectral absorbances of hyperbaric oxygen and hemoglobin make peak-and-valley crossovers at around 530- to 580-nm wavelengths (13). Thus, we employed 2-dimensional correlation analysis and evaluated the relationship between these wavelengths and 525-nm spectral features. Our findings at 525 nm were not affected by blood absorption (data not shown). Consequently, we were able to handle 525-nm spectral features as independent information. We obtained similar results for the resected specimens. In Study 1 (*in vivo* experiment), we observed only three colorectal cancers, but the 525-nm spectral features in colorectal cancer were supplemented by 21 cases of resected specimen observations. In the supplemental study, bloodless resected specimens were prepared to examine the 525-nm peak, and transition of the 525-nm peak was observed even when the blood had been removed from the specimen.

We particularly focused on the difference between the spectral data of normal mucosa and lesions within the same patient. All cases of 525-nm featured absorption were detected among the 21 cases of extracted tissue observations. The series of experiments included characteristics of each disease case (type of disease, stage, and individual differences).

The demonstrated sensitivity and specificity mentioned in this report represent one feasibility study for spectral detection and diagnosis because of the uncertainty of the 525-nm featured peak. Details of the 525-nm spectral features should be strictly examined, and correlations among spectral features, textures, and chemical components concerning the disease should be considered.

It is possible that spectral features are caused by cellular and subcellular structural changes and chemicals derived from metabolism (8). We are currently focusing on the relationship between 525-nm featured absorption and pathology and analyzing the cause of 525-nm featured absorption using microscopy–spectroscopy and chemical analysis.

Ultimately, the clinical success of each method of optical biopsy depends on the extent of additional improvements in detection sensitivity and specificity and on instrument cost. In addition, accurate histological validation of these techniques must be performed and can be achieved using endoscopes equipped with dual-instrument channels for proper registration of optical and standard punch biopsies. Kiyotoki *et al*. (14) measured hyperspectral data of gastric cancer using a fiber probe and obtained a sensitivity of 76.2% and specificity of 78.8% for the diagnosis of gastric adenocarcinoma.

Fluorescence endoscopy has been a leader in the area of spectral technology and offers the advantage of wide-area surveillance; however, artifacts may be introduced by the presence of metabolic changes such as inflammation,

ischemia, and hemorrhage. In addition, structural changes such as collagen thickening in polypoid lesions may crowd out sources of endogenous fluorescence. Our system has the potential to extend wide-band spectroscopy by changing its light source and can adapt to various spectral features. This means that a system of this type has the possibility of establishing new clinical diagnostic criteria based on true reflectance spectroscopy. In this article, we also demonstrated the feasibility of an endoscopic spectroscopy system with augmented reality image availability in the clinical setting.

Our system provides calibrated data acquisition within 30 sec. The whole procedure, including data analysis and visualization, can be concluded within 1 min, which is within the permissible time period during endoscopic examination. The spectral collection and diagnostic abilities of the system will be improved in our future system.

In conclusion, we developed an *in vivo* diagnostic system with hyperspectral analysis. Hyperspectral endoscopy has the potential to allow for real-time, noninvasive diagnosis of gastrointestinal diseases. New diagnostic criteria may be established based on the data of reflectance spectroscopy.

The results presented herein show that the intensity of reflectance spectra may have the ability to discriminate normal from abnormal conditions of the colonic mucosal tissue. Spectral peaks around 525 nm are specific to proliferative lesions. Our findings in colonic tissue compare well with the findings of previous groups. We believe that this endoscopic system will play a very important role in diagnosis of colorectal malignant lesions and will contribute to improvement in clinical outcomes in the field of gastroenterology.

Conclusion

We determined the specific spectral change in colorectal tumors by non-invasive HSC measurement. Real-time tumor mapping based on hyperspectral analysis is not only useful for assistance of the endoscopic diagnosis, but also assists in decision-making regarding resection of polyps in precancerous conditions.

Acknowledgements

The authors thank Prof. Hashizume, who provided carefully considered feedback and valuable comments. Special thanks also go to Prof. Maehara, whose opinions and information have helped very much throughout the implementation of this study.

References

1 Jemal A, Siegel R, Ward E, Hao Y, Xu J and Thun MJ: Cancer statistics, 2009. CA Cancer J Clin *59*: 225-249, 2009.

2 Pham TM, Fujino Y, Matsuda S and Yoshimura T: Premature mortality due to cancer in Japan, 1995 and 2005. Int J Cancer *127*: 190-194, 2010.

3 Liu Q: Role of optical spectroscopy using endogenous contrasts in clinical cancer diagnosis. World J Clin Oncol *2*: 50-63, 2011.

4 Utzinger U, Brewer M, Silva E, Gershenson D, Blast RC Jr., Follen M and Richards-Kortum R: Reflectance spectroscopy for *in vivo* characterization of ovarian tissue. Lasers Surg Med *28*: 56-66, 2001.

5 Bigio IJ and Bown SG: Spectroscopic sensing of cancer and cancer therapy: current status of translational research. Cancer Biol Ther *3*: 259-267, 2004.

6 Mehl PM, Chen Y-R, Kim MS and Chan DE: Development of hyperspectral imaging technique for the detection of apple surface defects and contaminations. Journal of Food Engineering *61*: 67-81, 2004.

7 Sambongi M, Igarashi M, Obi T, Yamaguchi M, Ohyama N, Kobayashi M, Sano Y, Yoshida S and Gono K: Analysis of Spectral Reflectance Using Normalization Method from Endoscopic Spectroscopy System. Optical Review 9: 238-243, 2002.

8 Lu G and Fei B: Medical hyperspectral imaging: a review. J Biomed Opt *19*: 10901, 2014.

9 Kawabata T, Mizuno T, Okazaki S, Hiramatsu M, Setoguchi T, Kikuchi H, Yamamoto M, Hiramatsu Y, Kondo K, Baba M, Ohta M, Kamiya K, Tanaka T, Suzuki S and Konno H: Optical diagnosis of gastric cancer using near-infrared multichannel Raman spectroscopy with a 1064-nm excitation wavelength. J Gastroenterol *43*: 283-290, 2008.

10 Dhar A, Johnson KS, Novelli MR, Bown SG, Bigio IJ, Lovat LB and Bloom SL: Elastic scattering spectroscopy for the diagnosis of colonic lesions: initial results of a novel optical biopsy technique. Gastrointest Endosc *63*: 257-261, 2006.

11 Koenig F, Larne R, Enquist H, McGovern FJ, Schomacker KT, Kollias N and Deutsch TF: Spectroscopic measurement of diffuse reflectance for enhanced detection of bladder carcinoma. Urology *51*: 342-345, 1998.

12 Ge Z, Schomacker KT and Nishioka NS: Identification of Colonic Dysplasia and Neoplasia by Diffuse Reflectance Spectroscopy and Pattern Recognition Techniques. Appl Spectrosc *52*: 833-839, 1998.

13 Jeon KJ, Kim SJ, Park KK, Kim JW and Yoon G: Noninvasive total hemoglobin measurement. J Biomed Opt *7*: 45-50, 2002.

14 Kiyotoki S, Nishikawa J, Okamoto T, Hamabe K, Saito M, Goto A, Fujita Y, Hamamoto Y, Takeuchi Y, Satori S and Sakaida I: New method for detection of gastric cancer by hyperspectral imaging: a pilot study. J Biomed Opt *18*: 26010, 2013.

Received December 14, 2015
Revised June 1, 2016
Accepted June 21, 2016